Journal of Orthopaedic Research
5:348–355, Raven Press, Ltd., New York

Surface Strain on Human Intervertebral Discs

Ian A. F. Stokes

Department of Orthopaedics and Rehabilitation, University of Vermont, Burlington, Vermont, U.S.A.

Summary: The biomechanical functions of the internal components of the intervertebral disc are not well understood. The surface deformation of 17 human cadaveric lumbar intervertebral discs was studied by photogrammetry by adhering small optical targets to the disc surface and thereby recording the length, bulge, and vertical height of lines on the disc surface representing annular fibers. Discs were studied in pure compression, flexion and extension, axial rotation, and shear. Two definitions of a fiber were investigated: first with the end-points of the fiber on the vertebra ("bone-to-bone" definition), second, where the end points of the fiber were just before the disc vertebra junction (the "disc-only" definition). Measurements were compared with a "constant-volume" physical model and with a mathematical model of the intervertebral disc. Fiber strains were 6% or less under physiological conditions. Comparison of results from the two definitions of fiber length showed greater strains for the disc-only definition in compressive loading. Fiber strains were less than in the constant-volume model of comparable dimensions in compressive loading by a factor of about two, thus suggesting fluid loss or end-plate deformations in the physiologic conditions. The mathematical model indicated that the surface strain for intervertebral discs is very sensitive to the disc-height: diameter ratio and to fluid loss from the disc but is less sensitive to the helix angle of the fibers. **Key Words:** Intervertebral disc—Biomechanics—Photogrammetry—Modeling—Degeneration—Strain.

The intervertebral disc is a unique anatomical structure since it provides a flexible articulation between bones without the sliding motion associated with diarthroidal joints. Very large forces are transmitted through the spine (24), and there is a large range of motion (more than 20° in flexion and extension) across the disc (2). The disc is an avascular structure but has highly organized collagenous framework (17). It can be considered to consist of three parts: the cartilaginous end-plate, the gel-like nucleus pulposus, and the annulus fibrosus, which is divided into multiple layers of crisscrossed fibers (12,27).

The intervertebral disc has been implicated in painful disorders of the spine, although it is probably an oversimplification to consider all back pain to be related to disc herniation or disc bulging (36). The bulk of the disc does not have a nerve supply although the periphery of the annulus and the end-plate are innervated (18). Age-related degenerative changes in the disc have been reported by Coventry et al. (8), Hirsch and Schajowitz (14), and Friberg and Hirsch (10), among others. These changes may be related to mechanical forces and deformations. Mechanisms of injury to the intervertebral disc have been studied in anatomical specimens. Pure compression of the spine usually produces fractures of the vertebral body or failure of the vertebral end-plate (28,32). Adams and Hutton (1) produced a central disc herniation in lumbar intervertebral discs subjected to a combination of compression and hyperflexion. The strain in annulus fibrosus at failure is of the order of 25% deformation

Address correspondence and reprint requests to Dr. I. A. F. Stokes, Department of Orthopaedics and Rehabilitation, University of Vermont, Burlington, VT 05405, U.S.A.

(11,37). It is not clear which forces acting on the disc and which deformations of the intervertebral disc may place it at risk for mechanical damage. Experimentally, axial torsion produces tears and fissures in the annulus (9). Mathematical models of the intervertebral disc structure have been used to predict the distribution of stress and strain in response to external loadings and deformation (3,5,6,21,22,33,34). These theoretical models, combined with measurements of intradiscal pressure (25,26,29), confirm that the intervertebral disc is a structure that supports compressive load by generation of high pressure within the radially confined nucleus pulposus.

The annulus fibrosus contains fibers that are aligned at approximately 57° to the axial direction (13). With compression of the intervertebral disc, the two ends of a fiber come closer together. At the same time, bulging of the disc (30) tends to elongate each fiber. It is not known which of these effects predominates, although it is expected that annular fibers elongate if they are under tension produced by the internal pressure within the disc. Under torsional loading, alternate layers of annular fibers are subjected to either shortening or lengthening depending on their alignment relative to the direction of torsion.

In this study, direct experimental measurements of the dimensions of "fibers" in the surface layers of human lumbar intervertebral discs were measured by a stereophotogrammetric method. The objective was to study these hypothesized mechanisms of deformation of annular fibers during incremental compression, eccentric compression (to produce combined compression and either flexion or extension), axial torsion, and shear.

MATERIALS AND METHODS

Measurement of Disc Deformation

Sections of human lumbar spines were removed at autopsy, wrapped in three layers of polyethylene with intervening layers of paper to protect the plastic from puncture, and stored at −20°C until use. Twelve spines were used (Table 1), and these provided 17 disc specimens for testing. On the day of testing, the spines were thawed and divided into motion segments (each consisting of two vertebrae and the intervertebral disc and ligaments joining them together). In order to make a specimen consisting only of intervertebral discs and vertebral bodies, the pedicles were sawed through and the posterior elements were removed. The vertebrae were then embedded in end-fittings by casting them into a dimensionally stable dental plaster (Whipmix Corp., Louisville, KY, U.S.A.). Prior to embedding, three wood screws were driven into each vertebral body to improve the fixation in the plaster.

TABLE 1. *Details of 17 intervertebral discs from 12 spines tested in this study; grade was assigned according to the method of Galante (11)*

Spine	Cause of death	Age (yr)	Sex	Specimen	Anatomical level	Grade
1	CVA	71	F	1	L4/5	2
				2	L2/3	2
2	PE	68	F	3	L4/5	3
				4	T12/L1	3
3	CVD	65	M	5	L4/5	3
4	P	74	M	6	L4/5	2
				7	L2/3	2
5	CVD	66	F	8	L4/5	2
6	CVD	64	M	9	L3/4	3
7	CVD	74	M	10	L3/4	3
8	P	74	M	11	L4/5	3
9	LC	68	F	12	L4/5	2
10	CVD	72	M	13	L3/4	2
11	CVD	26	M	14	L4/5	1
				15	L2/3	1
12	CVA	33	F	16	L4/5	1
				17	L2/3	1

Key (cause of death): CVA, cerebral vascular aneurysm; CVD, cardiovascular disease; LC, lung carcinoma; PE, pulmonary embolus; P, pneumonia.

After testing of the specimens, the discs were cut through transversely, and they were graded for their state of degeneration according to the method of Galante (11) (Table 1).

A method described previously (35) was used for measurement of surface deformation. Firstly, four "fibers" were marked on each intervertebral disc. Each fiber was located by examining the intervertebral disc surface by eye for a predominant fiber direction. A helical line in the clockwise and counterclockwise direction was marked by placing miniature optical targets along its length (Fig. 1). This was done in a central anterior location on the disc and on a posterior-lateral location between the sawn-off pedicles. These targets were adhered to the intervertebral discs by first coating the disc with a thin layer of petroleum jelly. This greasy coating served not only as an adhesive for the photographic targets but also as a way of conserving moisture within the disc. In this respect, the method was similar to that described by Hoffman

FIG. 1. One of a stereo pair of photographs of an intervertebral disc undergoing testing. This photograph shows two fiber directions marked by miniature optical targets for measurement purposes. Three larger target points mounted on each of the plaster embedded vertebrae were used to record relative motion of the vertebrae.

and Grigg (15). Specimens were tested at room temperature (20°C). A small fluorescent tube mounted between the cameras provided illumination but minimized heating of the specimens.

Four types of loading of intervertebral disc specimens were investigated: compression, bending, axial rotation, and shear. Compressive loading was applied to specimens mounted in a single-axis servohydraulic testing machine (Model 440, MTS Corp., Minneapolis, MN). First, an axis of the intervertebral disc was found experimentally by loading at different points on the top end-fitting until the disc was assessed visually as deforming in pure compression. The specimen was then locked in this position for testing. The deformation rate was 7.5 mm/min to a maximum ram motion of 2 mm. Stereo photographs were taken during both loading and unloading at intervals of approximately 0.4 mm of vertical compression.

To obtain bending, offset compression was applied at a point either 5 mm in front of or 5 mm behind the point at which pure compression deformation resulted. In the case of anterior fibers, this loading produced flexion or extension. For posterior-lateral fibers, the application of force was moved toward and away from this site, thus producing a combination of flexion and lateral bending motion. The rate of ram travel was again 7.5 mm/min. The ram displacement was reversed when it reached 2 mm.

Shear forces were applied by dead weights hung from a cable running over a pulley. The point of application of the force was adjusted vertically to insure by visual checking that the motion of the upper vertebra was in a horizontal plane. Loads were added in increments of 45 N up to 225 N.

Axial rotation was applied by means of a torque applied to the specimen through equal and opposite forces in cables attached to dead weights and running over pulleys. Pure axial rotation was maintained by positioning a flat platten over the upper end-fitting with a minimal force to prevent flexion and extension or lateral bending. Torque was added in increments of 3 N-m up to a maximum of 15 N-m.

The developed films were projected onto a Summagraphics digitizing tablet interfaced to a Digital Equipment Corporation PDP 11 computer for digitizing and analysis by a photogrammetric program (23). Dimensions of each fiber were measured as the total length, the bulge, and the total height, as shown in Fig. 2. In each loading state of the specimen, these dimensions were compared with the values in the unloaded state. This gave three measurements of disc surface deformation: the fiber elongation or strain (change in length divided by the original length, expressed as a percentage with positive values signifying increased fiber length); the bulge (difference in the bulge dimension, in millimeters, with positive values indicating increased bulge); and the compression (difference in the height dimension, also measured in millimeters, with positive values signifying compression). The

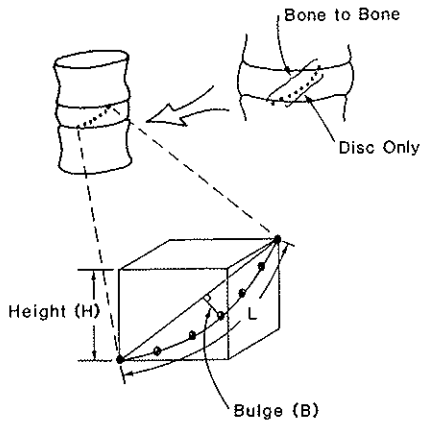

FIG. 2. Three measurements of the disc surface fiber dimensions. These are fiber length (L), from which percentage of elongation (or strain) was measured; bulge (B); and disc height (H), from which incremental compression was calculated. On the disc surface, "fibers" were marked from bone to bone. However, in the analysis of measurements, the fiber length could be truncated by omission of the first and last markers, thus giving two measures of the fiber deformation based on the bone-to-bone length and the disc-only length.

standard deviation of the measurements of fiber length was ±0.05 mm, giving an expected maximum error (95% confidence) of about ±0.15 mm (35), corresponding to a strain of about ±1% for a fiber of length 15 mm.

In the analysis of measurements of fiber deformation, two measurements of fiber length were used: first, the full length from bone to bone and, second, the "trimmed" fiber (with omission of the end-markers) to give the soft-tissue-only component of the disc deformation (Fig. 2).

Physical Models

In order to help with the interpretation of measurements from the human discs, physical models of the intervertebral disc were constructed. Three models of different dimensions were constructed and tested. The models were simplified by having cylindrical form. The combinations of disc dimensions used were diameter, 32 mm and height, 13.5 mm; diameter, 72 mm and height, 29 mm; and diameter 72 mm and height, 19 mm. The models consisted of two pieces of wooden dowel with a constant-volume intervertebral disc fabricated by filling part of a surgeon's glove with water, tieing it off, and then inserting it in a section of bicycle or motorcycle inner tube to represent the elastic annulus. A metal band (hose clamp) was used to bind the rubber inner tube to the dowel. The surface of the "disc" was marked with photographic targets as in the case of the human disc. The model discs were tested in compression, shear, and torsion.

Mathematical Model

An axisymmetrical (cylindrical) mathematical model was used to study geometric behavior of the disc surface. The model, which was an implementation of the geometry used in the model of Broberg and von Essen (5), consisted of a disc with a fluid (incompressible) nucleus surrounded by elastic components (fibers) connected to the rigid end plates and taking a helical path from one end plate to the other, with no bulge initially (i.e., it was cylindrical). Subsequently, the program calculated the change in the geometry of the disc as successive small deformations were imposed. The shape of the bulging surface of the disc was assumed to have a circular profile. At each increment of deformation, the amount of bulge that would give the required new volume (normally the same as the initial volume) was calculated iteratively. Then the fiber length was calculated by summating the distance from one end to the other, taking into account the bulging helical path. Results were expressed in the same format as for the measurements of the human discs (disc height and compression, fiber length and strain, and absolute and incremental disc bulge). The model was programmed for either compressive or torsional deformations.

RESULTS

Examples of strain-deformation graphs are shown in Figs. 3–6 for tests with compression, offset compression, shear, and torque loadings, respectively. Each test was characterized by the maximum values of the deformations associated with it. In each type of applied loading, the deflection in the direction of the applied deformation (compression, flexion/extension, shear motion, and torsion) was used as the independent variable against which the disc surface deformation was compared. In general, the maximum deflection was different for all specimens since it was the applied load that was controlled during each test.

Compression Loading

The mean compressive force applied to the disc specimens was 2.15 kN (standard deviation, 0.44 kN). The amount of bulge was greater at anterior locations than at posterior-lateral locations and was greater when measured from bone to bone than on the disc-only parts of the specimens (Table 2). The

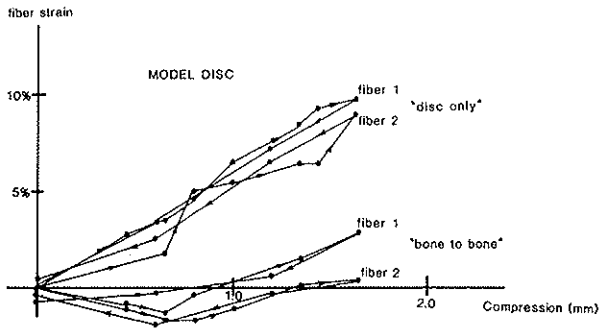

FIG. 3. Measurements of fiber strain during a compression experiment on the physical model disc (disc height, 13.5 mm; diameter, 32 mm) plotted against the compression of the disc measured at the vertebrae. The strain measurements were different for the two definitions of fiber length. A similar pattern of findings was obtained from the human disc specimens.

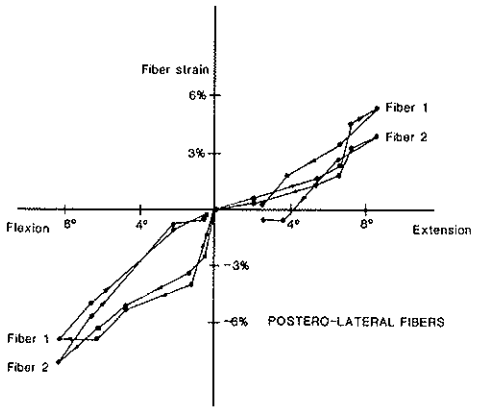

FIG. 4. Disc fiber strain (bone-to-bone definition) in flexion and extension testing of a human disc (#15) at the posterolateral site.

amount of vertical compression of the disc fiber measured photographically was less than the amount of the ram movement by a factor of more than two times. This was attributed to the flexibility of the vertebrae. This disparity was not found in the case of the physical model disc.

The amount of compression of the disc alone was less than the amount of compression measured from bone to bone by a factor of about two, and the surface strain was greater for the bone-to-bone definition of a fiber (Table 2). This disparity was also seen in the physical model disc (Fig. 3). The maximum strain (disc only) at the anterior site had a mean value of 1.73% at a compression (bone to bone) of 0.67 mm. At posterior-lateral sites, the maximum strain was 1.66% for 0.83 mm compression. Thus the strain:compression ratio was 2.6%:1

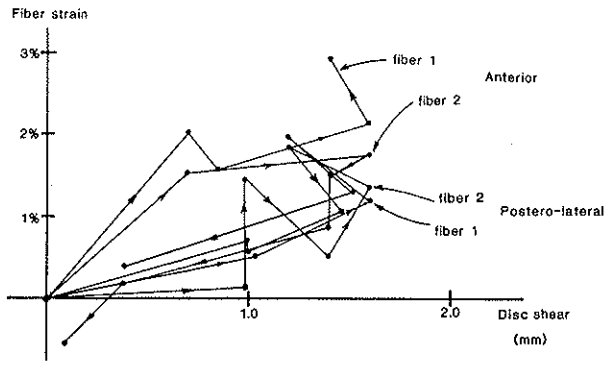

FIG. 5. Disc fiber strain in a human disc (#15) (bone-to-bone definition) in shear loading up to 225 N. These results are for the two fibers (clockwise and counterclockwise) at the anterior site and for the two fibers at the posterolateral site. Measured strains are comparable with the measurement accuracy (±1% strain).

mm (anteriorly) and 2.0%:1 mm (posterior-lateral sites). This compares with 5%:1 mm for the physical model (Fig. 3) and 3%:1 mm for the mathematical model without fluid loss (Fig. 7). The larger physical disc models had lesser surface strain for the same amount of compression. Decreasing the initial height of the larger disc model (from 29 mm to 19 mm) produced a marked increase in the measured strains from 2% to 8% at 1 mm compression. Fluid loss in compressive loading of the mathematical model disc predicted a progressive reduction in the disc surface strain and an increasingly nonlinear relationship to the disc compression (Fig. 7). In these experiments, the dimensions of the disc were 40 mm diameter and 10 mm disc height, which are the typical values for a human disc given by Hickey and Hukins (13). The same proportion of disc height:diameter gave the same surface strain per millimeter of compression. However, reducing the disc height from 10 mm to 8 mm predicted an increase in the surface strain (2.4%:1 mm to 4.7%:1 mm). Changing the fiber angle (helix angle to the axial direction) from 45° to 60° had the effect of increasing the calculated fiber strain by 1% or less for compression in the range of 0–2 mm.

Offset Compression

The offset compression of the specimens produced mean flexion or extension of ±6.5°. Extension (bending away from the measurement site) produced positive fiber strains (stretching), and flexion (bending toward the measurement site) produced negative strain. The absolute amount of surface strain measured in flexion was less than the strain (in the opposite sense) measured in extension experiments. Differences between the bone-to-bone and the disc-only measures were also present in these experiments, as was seen in the compression experiments. The differences were greater in the flexion experiments than in the extension experiments, and in the flexion (rotation toward the measurement site) the differences were consistent with those seen in compression experiments, in that the strain was less negative in the disc-only definition of a fiber (Table 1). In extension away from the measurement site, the surface strain was 0.6%:1° for both the large- and small-diameter physical disc models. In flexion, the strain was −0.6%:1° for the disc-only definition of a fiber, but it was less negative for the bone-to-bone definition, as was also seen in the human discs.

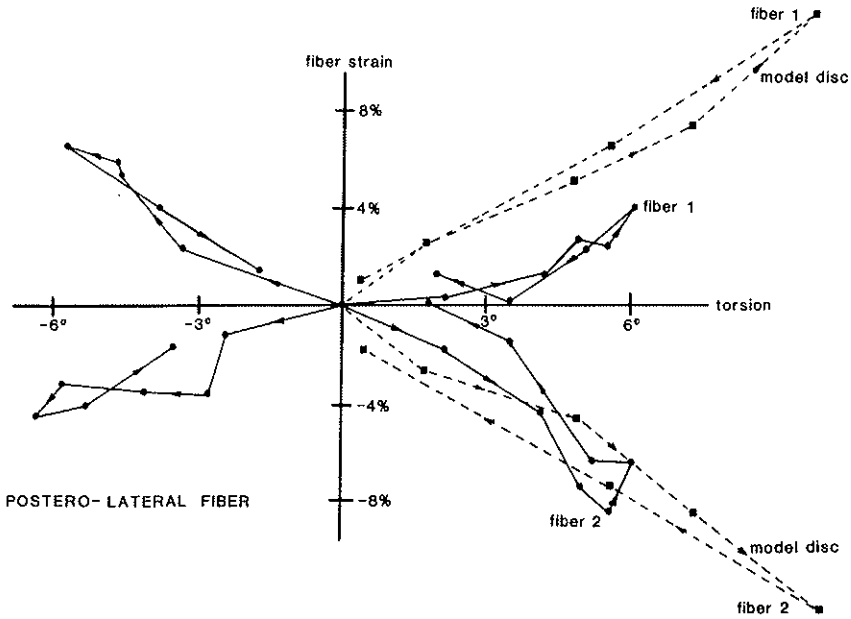

FIG. 6. Disc fiber strain (bone-to-bone definition) in torsional loading up to 15 N-m in clockwise and counterclockwise directions (measurements from posterolateral fibers) with results from the physical model disc superimposed. Strains in fibers 1 and 2 (which ran in opposite directions) were complementary.

Shear

The mean amount of shear motion produced was 2.38 mm at anterior sites and 2.03 mm at posterior-lateral sites. In shear, both the anterior and posterior-lateral sites showed positive strain (elongation), and the strain was not significantly different at the different sites. The difference between the bone-to-bone measure of strain and the disc-only measure was small (Table 2). In shear, the surface strain (for both definitions of a fiber) was 1%:1 mm for the smaller physical model disc and 0.5%:1 mm for the larger model.

Torsion

In the torsion experiments, both clockwise and counterclockwise tests were performed at each site, and there were two fibers marked at each site; hence, four measurements of fiber deformation were obtained from each site on each disc. The direction of the strains measured in counterclockwise fibers was opposite to that measured in clockwise fibers. Therefore, measurements from the fibers were pooled and averaged but only after correcting the sign of the strains according to the direction of the fiber. The mean torsion angle reached in these experiments (at 15 N-m applied torque) was 6.7°. At this maximum torsion, the fiber strains (normalized by both the amount of the torsion and the direction of the fiber) were significantly greater at posterior-lateral sites than at anterior sites, by a factor of about two times. There was no significant difference between the measurements of fiber strain

TABLE 2. *Summary of surface deformations of 17 intervertebral discs (mean and S.D.)*

	Maximum compression (mm)	Maximum compression bulge (mm)	Maximum compression strain (%)	Flexion strain (%/deg)	Extension strain (%/deg)	Shear strain (%/mm)	Torsion strain (%/deg)
Anterior fibers							
Bone-to-bone	0.67	0.82	0.80	0.46	0.76	0.46	−0.51
	(0.24)	(0.25)	(1.80)	(0.35)	(0.42)	(1.14)	(0.34)
Disc-only	0.32	0.55	1.73	0.07	0.59	0.47	−0.44
	(0.23)	(0.31)	(1.44)	(0.47)	(0.49)	(1.46)	(0.44)
Posterolateral fibers							
Bone-to-bone	0.83	0.58	−0.53	0.70	0.83	0.45	−0.84
	(0.33)	(0.36)	(2.46)	(0.50)	(0.64)	(1.46)	(0.43)
Disc only	0.42	0.41	1.66	0.27	0.51	0.24	−0.94
	(0.30)	(0.29)	(3.10)	(0.60)	(0.96)	(2.34)	(0.61)

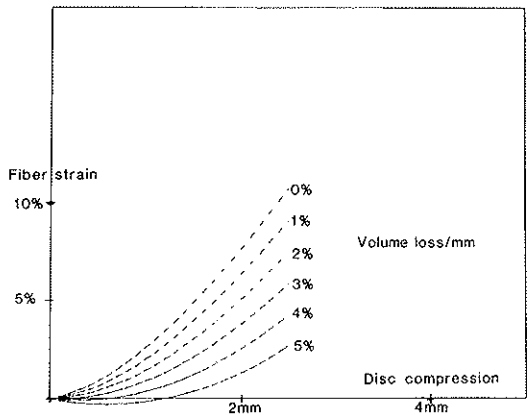

FIG. 7. Surface strain on the mathematical model disc (diameter, 40 mm; height, 10 mm) under compressive loading with varying amounts of fluid expelled from the disc during the compression. The percentage volume loss (0–5%) was that lost for each millimeter of compression.

based on the bone-to-bone measure compared with the disc-only measure (Table 2).

In torsion, both the physical and mathematical model disc strain was approximately 1%:1° of torsion, which was a little more than seen in the human discs. In the two physical model discs with the same diameter (72 mm), the disc strain was 1.4%:1° of torsion for the 19-mm-thick disc and 1%:1° of torsion for the thicker (29 mm) disc. Reducing the model disc height from 10 mm to 8 mm while holding the diameter constant at 40 mm predicted an increase in surface strain in torsion from 1.3%:1° to 1.7%:1°. Changing the fiber angle from 45° to 60° produced a decrease of less than 2% strain for torsion up to 5°.

DISCUSSION

The magnitudes of the loads and deformations applied to the specimens in these experiments were probably close to the physiological maxima. The compressive loads were of the order of 20% of failure loads (7,24). The amount of flexion and extension was about 60% of the maximum according to Allbrook (2). The torsion was greater than the physiological range described by Farfan et al. (9) because of the removal of the posterior elements. The amount of surface strain found under these loads and deformations was much less than the ultimate tensile strain of about 25% found by Galante (11) and by Wu and Yao (37). Adopting as the physiologic ranges 2 mm of compression, 8° of flexion and extension, 4° of torsion, and 2 mm of shear, then maximal strains would be about 4%, 6%, 4% and 1%, respectively. Thus, it appears that the normal physiological range of deformation of the surface of the disc does not place it at risk for tensile failure, based on the published measurements of the ultimate strain (11,37). However, this assumes that the initial length of specimens in the published studies in vitro corresponded to the resting length in vitro. In torsional loading experiments, there was a large difference in the strains in alternately aligned fiber directions. This latter effect may be the most important in terms of its potential for producing mechanical damage. In torsion, larger strains were measured in fibers at posterior-lateral sites compared with those at anterior sites. The posterior-lateral region is predicted to be one at risk for mechanical damage because of the lesser radius of curvature, and the symptomatic consequences of disc bulging and herniation at this site are more severe.

The findings in compressive loading were characterized by very little surface strain (as also indicated by the measurements of rabbit disc deformations by Klein et al. [20]) and very large differences in the measures obtained by the bone-to-bone and disc-only measures. Similar findings were obtained from the model discs, although in the models the magnitude of the surface strain was generally greater. The models had no end-plate deformation and no fluid loss (constant volume). This probably explains the difference between the model and experimental findings, since deformations of the end-plates are significant (4,32), and there is theoretical (33) and experimental (19) evidence suggestive of fluid loss from the disc with compression. The model of Broberg (6) predicts 5% surface strain per millimeter of compression, 0.4% per degree of flexion or extension, 1% per degree of shear, and 1% per degree of torsion. Thus, the measured strains were similar for flexion and extension, considerably less in compression, and about half those predicted for shear and for torsion at anterior sites.

The disparity between the three measures of compression made here (ram movement, bone-to-bone compression, and disc-only compression) suggests that the compression of intervertebral discs is associated with significant vertebral compression (31), deformation of the end-plate (4,16), and a complex pattern of deformation of the disc whereby the periphery of the disc does not compress as much as the approximation of the bony attachments to the end-plates. The difference be-

tween the bone-to-bone measures and the disc-only measures were also found in flexion and extension, but they were more pronounced in flexion (angulation towards the measurement site) than in extension. Thus, flexion, which produced compression of the disc at the measurement site, was more similar to the compression load findings in this respect. The reason for the difference between the two measures is not clear but it implies that strain is concentrated at the disc-vertebral junction. It is possible that this is related to spur and osteophyte formation at this site in degenerating discs.

Acknowledgment: Supported by NIH R01 AM30165. Valuable technical assistance was given by David M. Greenapple, Lisa Friedman, and Robert A. Lunn.

REFERENCES

1. Adams MA, Hutton WC: Prolapsed intervertebral disc: A hyperflexion injury. *Spine* 7:184–191, 1982
2. Allbrook D: Movements of the lumbar spinal column. *J Bone Joint Surg* 39B:339–345, 1957
3. Belytschko T, Kulak RF, Schultz AB, Galante JO: Finite element stress analysis of an intervertebral disc. *J Biomech* 7:277–286, 1974
4. Brinckmann P, Frobin W, Hierholzer E, Horst M: Deformation of the vertebral end plate under axial loading of the spine. *Spine* 8(8):851–856, 1983
5. Broberg KB, von Essen HO: Modeling of intervertebral discs. *Spine* 5(2):155–167, 1980
6. Broberg KB: On the mechanical behaviour of intervertebral discs. *Spine* 8(2):151–165, 1983
7. Brown T, Hansen RJ, Yorra AJ: Some mechanical tests on the lumbosacral spine with particular reference to the intervertebral discs. *J Bone Joint Surg* 39A(5):1135–1164, 1957
8. Coventry MB, Ghormley RK, Kernohan JW: The intervertebral disc: Its microscopic anatomy and pathology. Part I: Anatomy, development and physiology. *J Bone Joint Surg* 27(A):105–112, 1945.
9. Farfan HF, Cossette JW, Robertson GH, Wells RV, Kraus H: The effects of torsion on the lumbar intervertebral joints. The role of torsion in the production of disc degeneration. *J Bone Joint Surg* 52A:468–497, 1970
10. Friberg S, Hirsch C: Anatomical and clinical studies on lumbar disc degeneration. *Acta Orthop Scand* 19:222–242, 1949
11. Galante JO: Tensile properties of the human lumbar annulus fibrosus. *Acta Orthop Scand* [*Suppl*]100:55–66, 1967
12. Happey F: A biological study of the human intervertebral disc. In: *The Lumbar Spine and Back Pain*, ed by MIV Jayson, London, Sector, 1976, pp 293–316
13. Hickey DS, Hukins DWL: Relation between the structure of the annulus fibrosus and the function and failure of the intervertebral disc. *Spine* 5:106–116, 1980
14. Hirsch C, Schajowicz F: Studies on the structural changes in the lumbar annulus fibrosus. *Acta Orthop Scand* 22:184–231, 1953
15. Hoffman A, Grigg P: A method for measuring strains in soft tissue. *J Biomech* 17(10):795–800, 1984
16. Horst M, Brinckmann P: Measurement of the distribution of axial stress on the end-plate of the vertebral body. *Spine* 6(3):217–232, 1981
17. Inoue H: Three-dimensional architecture of lumbar intervertebral discs. *Spine* 6(2):139–146, 1981
18. Jackson HC, Winkelman RK, Bickel WH: Nerve endings in the human lumbar spinal column and related structures. *J Bone Joint Surg* 48A:1272–1281, 1966
19. Kazarian LE: Creep characteristics of the human spinal column. *Orthop Clin North Am* 6:3–18, 1975
20. Klein JA, Hickey DS, Hukins DWL: Radial bulging of the annulus fibrosus during compression of the intervertebral disc. *J Biomech* 16(3):211–217, 1983
21. Kulak RF, Belytschko TB, Schultz AB: Nonlinear behavior of the human intervertebral disc under axial load. *J Biomech* 9:377–386, 1976
22. Kulak RF, Schultz AB, Belytschko T, Galante J: Biomechanical characteristics of vertebral motion segments and intervertebral discs. *Orthop Clin North Am* 6(1):121–133, 1975
23. Marzan GT: *Rational design for close-range photogrammetry*. (Ph.D. Thesis, University of Illinois, 1975.) Xerox University Microfilms, Ann Arbor, MI, 1976
24. Morris JM, Lucas DB, Bresler B. The role of the trunk in stability of the spine. *J Bone Joint Surg* 43A:327–351, 1961
25. Nachemson A: The load on lumbar discs in different positions of the body. *Clin Orthop* 45:107–122, 1966
26. Nachemson A, Elfstrom G: Intravital dynamic pressure measurement in lumbar discs. *Scand J Rehabil Med* [*Suppl*] 1:13–25, 1970
27. Panagiotacopulos ND, Krauss WG, Bloch R: On the mechanical properties of human intervertebral disc material. *Biorheology* 16(4–5):317–330, 1979
28. Perey O: Fracture of the vertebral end-plate in the lumbar spine: An experimental biomechanical investigation. *Acta Orthop Scand* [*Suppl*] 25:49–68, 1957
29. Ranu HS, Denton RA, King AI: Pressure distribution under an intervertebral disc—An experimental study. *J Biomech* 12:807–812, 1979
30. Reuber M, Schultz A, Denis F, Spencer D. Bulging of lumbar intervertebral disks. *J Biomech Eng* 104:187–192, 1982
31. Rolander SD: Motion of the lumbar spine with special references to the stabilizing effect of posterior fusion. *Acta Orthop Scand* [*Suppl*] 90:61–63, 1966
32. Rolander SD, Blair WE: Deformation and fracture of the lumbar vertebral end plate. *Orthop Clin North Am* 6(1):75–81, 1975
33. Sonnerup L: A semiexperimental stress analysis of the human intervertebral disc in compression. *Exp Mech* 12:142–147, 1972
34. Spilker RL: Mechanical behavior of a simple model of an intervertebral disk under compressive loading. *J Biomech* 13:895–901, 1980
35. Stokes I, Greenapple DM: Measurement of surface deformation of soft tissue. *J Biomech* 18(1):1–7, 1985
36. Strange FGStC: Debunking the disc. *Proc R Soc Med* 59:952–956, 1966
37. Wu H-C, Yao R-F: Mechanical behavior of the human annulus fibrosus. *J Biomech* 9:1–7, 1976